JTTEE5 20:252–259
DOI: 10.1007/s11666-010-9533-9
1059-9630/$19.00 © ASM International



# Investigation of Impact Behavior of Cold-Sprayed Large Annealed Copper Particles and Characterization of Coatings

*Wenya Li, Xueping Guo, Min Yu, Hanlin Liao, and Christian Coddet*

*(Submitted May 4, 2010; in revised form June 24, 2010)*

**In this research, the large gas-atomized copper powder was selected as the feedstock. Some powder was annealed in a vacuum circumstance to avoid the effect of grain boundaries on the high velocity impact behavior of particles during cold spraying. The annealed Cu powder was deposited by cold spraying with respect to the single impacts and coating deposition under certain gas condition. In addition, the rebounded copper particles were collected for morphology analysis compared to the adhered particles. The results show that the average size of the rebounded particles is apparently increased compared with the starting powder because of the rebounding of larger particles and intensive plastic deformation of the rebounded particles. For the deposited particles, obvious plastic deformation causes a higher hardness to the coating. It is found that the rebounded particles have also experienced large deformation and shear instability at the impact interfaces.**

**Keywords** annealing, cold spraying, copper, high velocity impact behavior, microstructure

## 1. Introduction

Cold spraying is a coating technique on the basis of aerodynamics and high-speed impact dynamics. In this process, spray particles are accelerated to high velocity by a high-speed gas flow that is generated through a convergent-divergent nozzle. A coating is usually formed through the intensive plastic deformation of particles impacting on a substrate at a temperature well below the melting point of the spray material (Ref 1). In the last decade, this spraying technique has been widely investigated by both experimental and numerical methods owing to its advantages over the conventional thermal spray processes to deposit a wide variety of metals, alloys, and composites (Ref 2).

Although it has great application potentials in aerospace, automobile manufacture, chemical industry, etc., there are still some important aspects to be well revealed including the actual bonding mechanism of spray particles. The most prevailing hypothesis is that plastic deformation may disrupt thin surface films, such as oxides, and provide intimate conformal contact under high local pressure, thus permitting bonding to occur, and thus, this bonding process was considered to be comparable to that in explosive welding or shock wave powder compaction (Ref 3, 4). The above-mentioned bonding hypothesis is consistent with the fact that a wide range of ductile materials, such as metals and alloys, have been deposited by cold spray and that the spray particles experience extensive deformation to form lens-like shapes. Non-ductile materials, such as ceramics, can only be deposited if they are co-cold-sprayed with a ductile (matrix) material or sprayed on a ductile substrate to form a thin layer. This hypothesis can also explain the observed critical velocity necessary to achieve a successful deposition (Ref 5). This critical velocity was demonstrated to be influenced by the particle size (Ref 6), temperature (Ref 4-7), and its oxidation state (Ref 7-9) besides the mechanical properties of given particle and substrate materials (Ref 1, 2).

The reported numerical results (Ref 3-7, 10, 11) indicated that the temperature at the localized contact interfaces rises remarkably due to the possible adiabatic shear process. Through numerical simulations by ABAQUS software, Assadi and co-workers (Ref 4, 6, 12) found that the instability of adiabatic shear flow occurs as particle

This article is an invited paper selected from presentations at the 2010 International Thermal Spray Conference and has been expanded from the original presentation. It is simultaneously published in *Thermal Spray: Global Solutions for Future Applications, Proceedings of the 2010 International Thermal Spray Conference*, Singapore, May 3-5, 2010, Basil R. Marple, Arvind Agarwal, Margaret M. Hyland, Yuk-Chiu Lau, Chang-Jiu Li, Rogerio S. Lima, and Ghislain Montavon, Ed., ASM International, Materials Park, OH, 2011.

**Wenya Li** and **Min Yu**, Shaanxi Key Laboratory of Friction Welding Technologies, Northwestern Polytechnical University, Xi'an 710072, People's Republic of China; **Xueping Guo, Hanlin Liao,** and **Christian Coddet**, LERMPS (Laboratoire d'Etudes et de Recherches sur les Matériaux, les Procédés et les Surfaces), Université de Technologie de Belfort-Montbéliard, Site de Sévenans 90010, Belfort Cedex, France; and **Xueping Guo**, Marine Engineering College, Dalian Maritime University, Dalian 116026, Liaoning Province, People's Republic of China. Contact e-mail: liwy@nwpu.edu.cn.

velocity becomes higher than a threshold. They proposed a hypothesis stating that the adiabatic shear instability could be responsible for the bonding of particles in cold spraying. Based on the modeling of impact of copper particles, they concluded that bonding of particles can be attributed to the adiabatic shear instability occurring at the interfaces of particles and/or substrate. Therefore, they took the velocity at which the impacting particles can achieve shear instability as the actual critical velocity for particle deposition in cold spray (Ref 4, 6, 12). However, owing to the excessive distortion of meshing at the local contact zones in simulations by the Lagrangian algorithm, this calculated critical velocity is much dependent on the meshing size (Ref 7, 11, 13). Therefore, whether the simulated critical velocity can be taken as the real one requires some further investigation. Based on much experimental and simulation work, the authors attempt to discuss whether the simulated shear instability can be associated directly with the actual shear instability upon particle impacting, by taking the element distortion in simulations into account. In addition, another question arises: Does the observed real critical velocity have any relationship with the shear instability during impacting? To answer the above query, the large annealed gas-atomized copper powder was selected as the starting spray material. The experiment design was based on the single impacts and coating deposition.

## 2. Experimental Procedure

A sieved gas-atomized Cu powder (−120 + 150 mesh, LERMPS Lab, France) was selected as the feedstock. As shown in Fig. 1, the starting Cu particles present a spherical morphology with the equiaxed grains of the order of ten microns. Some powder was annealed at 700 °C for 24 h in a vacuum circumstance to soften the particles to the greatest extent. The powder size distribution was characterized by a laser diffraction sizer (MASTERSIZER 2000, Malvern Instruments Ltd., UK). The cold-rolled Cu plates (5 mm thick) were polished and heat treated under the same condition as the annealed powder.

A cold-spray system with a commercial cold spray gun (CGT GmbH, Germany) was employed for coating deposition. An optimized round nozzle design was adopted, which had an expansion ratio of about 4.9 and a divergent section length of 170 mm. High-pressure compressed air was used as the accelerating gas, and argon was used as powder carrier gas. The spraying was conducted with an air inlet pressure of 2.7 MPa and temperature of about 513 °C. The pressure of argon was about 2.9 MPa. The standoff distance from the nozzle exit to the substrate surface was 30 mm. The traverse speed of spray gun was 1000 mm/s for single impacts, and 100 mm/s for coating deposition. Particle velocity prior to impacting was estimated according to the spray parameters by using the developed 2D axisymmetrical model with the FLUENT software (Ref 14).

The powder and coating microstructures were examined by optical microscope (OM) (Nikon, Japan), SEM (JSM5800LV, JEOL, Japan). Some cross-sectional samples were eroded with an aqueous solution composed of 5 g $FeCl_3$ + 10 mL HCl + 100 mL $H_2O$. The coating microhardness was tested by a Vickers hardness indenter (Leitz, Germany) with a load of 300 g for 15 s, while the particle hardness was measured with a load of 100 g. More than 15 values were randomly tested and averaged to evaluate the hardness.

## 3. Results and Discussion

### 3.1 Powder Characterization

Figure 2 shows the measured particle size distribution of the annealed Cu powder. The average size of the annealed powder is about 99 μm, which is a little larger than that of the starting Cu powder. In addition, the size range of the annealed powder is also broader than that of the starting Cu powder with more large particles. Some particles may be inevitably sintered to form the larger ones, as can be observed during the SEM observation of the annealed powder as shown in Fig. 3.

The annealed Cu powder was mounted and polished for the observation of the particle cross section as shown in Fig. 4. The oxygen content of the original powder (i.e., before annealing) could be about 0.01 wt.% according to the previous measurement (Ref 7); however, the annealed particles shown in Fig. 4 seem to have a little lower oxygen content, which could be explained by the degassing

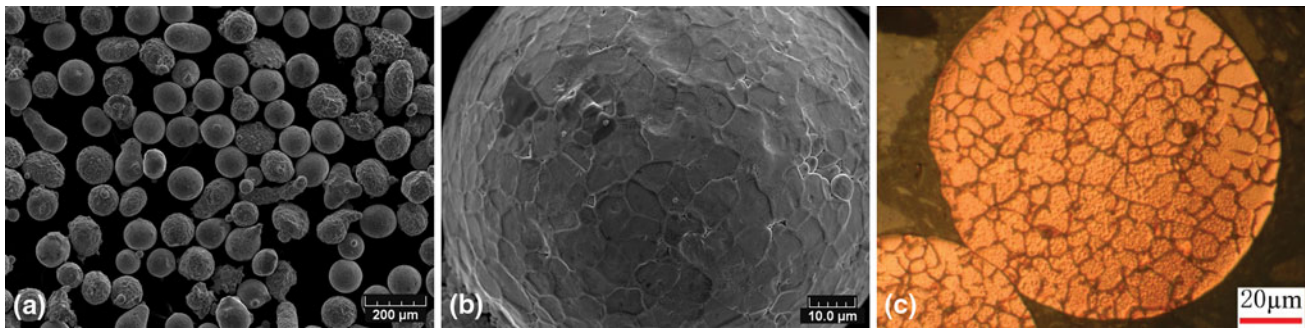


**Fig. 1** SEM morphology of the starting Cu powder (a) and a particle (b), and OM micrograph of a particle cross section (c)

effect during the powder heat treatment process. It is seen from Fig. 4(b) that the grains within the particles has obviously grown up to several tens of microns with many twins present after the annealing treatment compared with the starting powder particles (Fig. 1c). This can also be found as comparing Fig. 1(b) with Fig. 3(b).

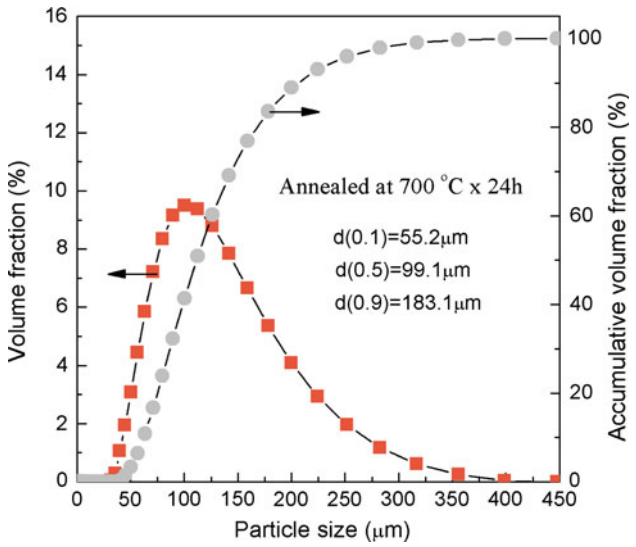


**Fig. 2** Size distribution of the annealed Cu powder

Particle velocity estimation was conducted with the developed 2D axisymmetrical model using FLUENT software (Ref 14). The results are shown in Fig. 5. It is seen that although the size distribution of the annealed powder is relatively broad, the velocities of most particles range from 280 to 400 m/s. The average particle velocity for the annealed powder is about 340 m/s. According to Eq 1 proposed by Schmidt et al. (Ref 6), for achieving a sufficiently slow thermal diffusion, a minimum particle diameter corresponding to this velocity can be estimated to be 12.4 μm, which is much smaller than the measured mean particle size of the annealed powder as shown in Fig. 1. It should be noted that this critical diameter can only be used as an estimation of the size of a given particle required to obtain a successful bonding. It can be influenced by other factors such as the temperature, the oxide content, the impact angle of particles, and the mechanical properties of substrate.

$$d_{\text{critical}} = 36\frac{\lambda}{C_p \rho v_{\text{particle}}} \qquad \text{(Eq 1)}$$

Nevertheless, it seems that this particle velocity of 340 m/s will not be satisfactory for particle deposition of the annealed large particles if the critical velocity of Cu

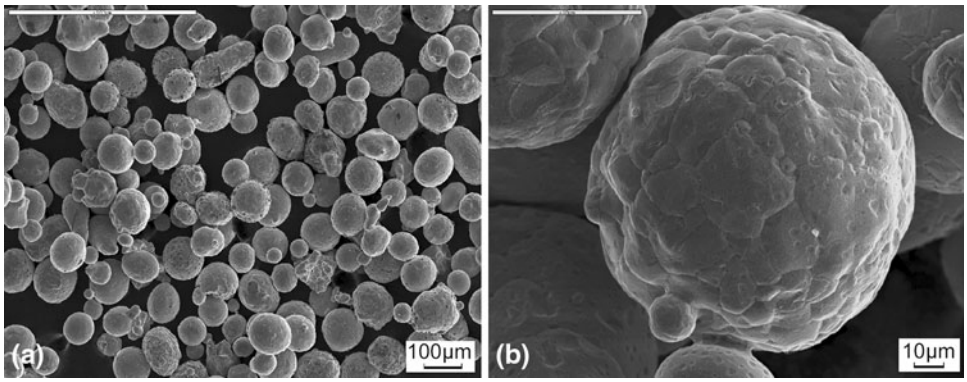


**Fig. 3** SEM morphology of the annealed Cu powder (a) and a particle (b)

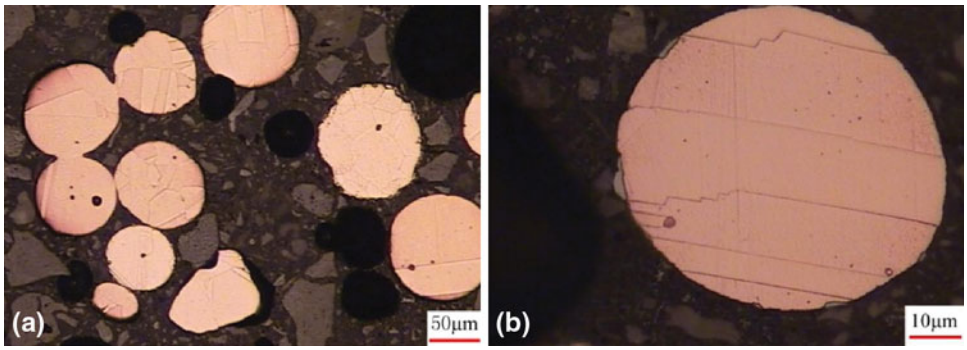


**Fig. 4** OM micrographs of the cross section of the annealed Cu powder (a) and a particle (b)

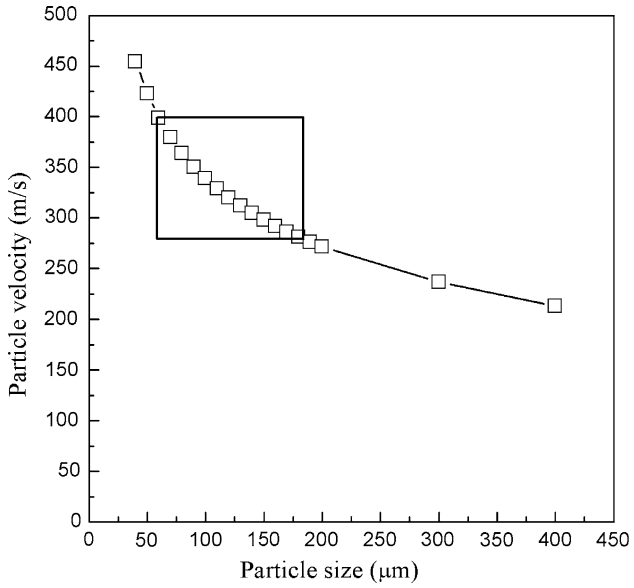


**Fig. 5** Calculated particle velocity before impact with the developed 2D model using FLUENT (Ref 13). Note that the frame inside this figure stands for the particle size and velocity window

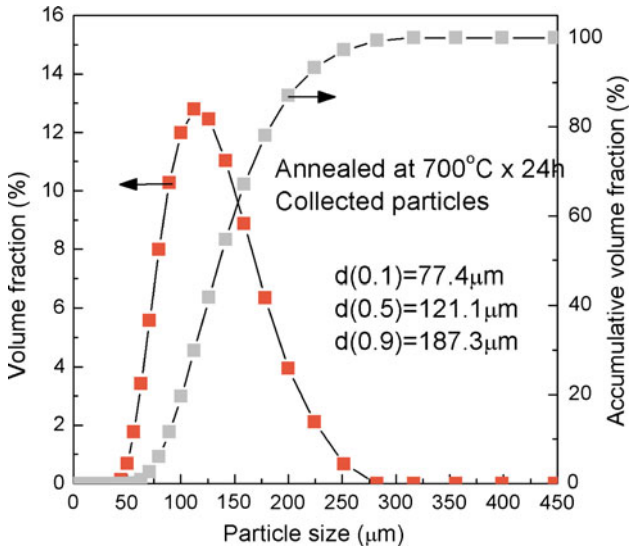


**Fig. 6** Size distribution of the collected Cu particles after coating deposition with the annealed powder

particle is larger than 400 m/s as reported by Schmidt et al. (Ref 6).

### 3.2 Impacting Behavior of Particles

**3.2.1 The Rebounded Particles.** To investigate the particle impacting behavior, the rebounded particles were collected and analyzed. Figure 6 shows the measured size distribution of the collected particles for the annealed powder after coating deposition. It is found that the average particle size of the annealed powder has increased after particle impacting, which is about 121 μm compared to about 99 μm before impacting. It could be considered that two important reasons cause this increase in the apparent particle size. One is because of the flattening of the impacting particles as can be clearly seen from the particle morphology (Fig. 7). Another reason is that the rebounded or unbonded particles are possibly large and thus have a relatively low impacting velocity compared to the existing critical velocity. Nevertheless, some particles have been successfully deposited onto the substrate and formed a coating, which suggests the critical velocity for these particles is believed to be less than 400 m/s. This value is lower than the reported critical velocities for Cu powder by other researchers (Ref 1-6) and consistent with our previously observed result (Ref 7). This also confirms that coarse particles can have a lower critical velocity (Ref 6, 12).

To answer the question that whether the rebounded particles have experienced the shear instability during impacting, the collected powder was observed using SEM. The results are shown in Fig. 7. It is very interesting to find that most particles for both single impacts and coating deposition have experienced large plastic deformation to form lens-like shapes. The existence of some evidence clearly proves the occurrence of shear instability for those rebounded large particles, as indicated by the zones marked by the circles in Fig. 7. Some excellent simulation work with regard to the impacting and bonding process of particles has been conducted. It has been considered in the literature that the bonding of particles occurs initially at the edge of the contact zones (Ref 6, 12, 15, 16). This has been ascribed to the sufficiently high shear strain induced by high pressure gradient between impacting interfaces, which could ultimately cause adiabatic shear instability (Ref 6). From Fig. 7, we cannot tell whether the zones, which experienced shear instability, are just the rim of particle during impacting. It is possibly the case for Fig. 7(b), however, for Fig. 7(a), the marked zone seems more like the bottom of an impacting particle.

The obtained results seem to positively support the conclusion that shear instability does not necessarily lead to particle bonding. Schmidt et al. have performed a series of macro-impact experiments by impinging 20-mm copper and carbon steel balls onto a substrate (Ref 6) whose experimental results demonstrated that the steel ball impacted at a velocity of 460 m/s and bounced back from the substrate; however, the outer rim of the impact crater presented ductile fracture, whereas the bottom of the crater showed no sign of shear instability. Results obtained in this study and the literature (Ref 6) confirm that shear instability could only be a precondition for a successful bonding of a particle, rather than an inevitable one.

**3.2.2 Surface Morphology.** Figure 8 shows the surface morphology of the substrate after single impacts. It is clearly seen from Fig. 8(a) that many particles are adhered to the substrate even through a single scanning of spray nozzle. This may suggest the deposition efficiency under the present gas conditions could be relatively high. When observed at high magnification, the obvious jetting

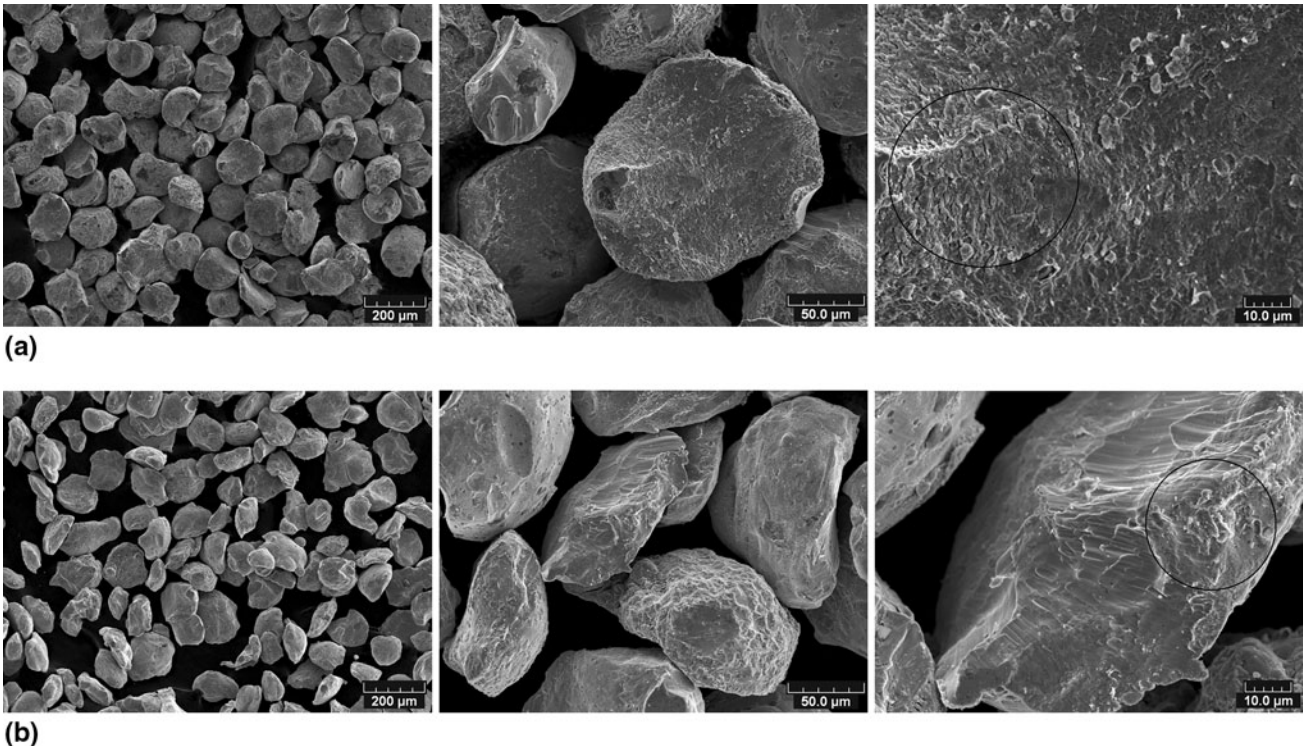


**Fig. 7** SEM morphology of the annealed Cu powder collected after single impacts (a) and coating deposition (b)

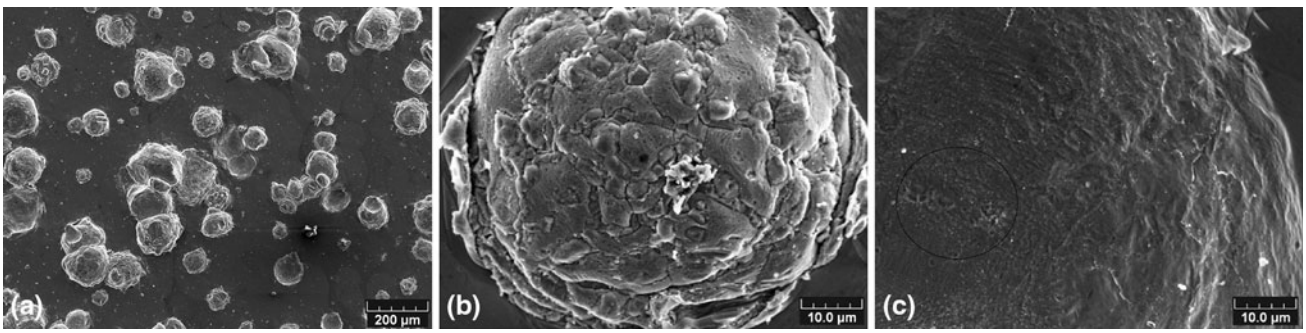


**Fig. 8** Surface morphology of the substrate after single impacts (a). (b) An adhered particle and (c) a crater

presents in the periphery of the adhered particles as shown in Fig. 8(b). This phenomenon is consistent with previous studies (Ref 4, 6, 12, 16). However, severe shear can also be found at the impacted surfaces for the unbonded particles as shown in Fig. 7. It has been considered that the bonding induced by shear instability is more likely to occur at the particle periphery (Ref 12, 16, 17) and that there will never be a shear instability occurring at the most bottom region of particle although the maximal pressure could be built up there (Ref 12). However, it is very interesting to find that some evidence of bonding and rebounding presents at the bottom of the crater created in the substrate marked by the circle as shown in Fig. 8(c). The question of whether a particle sticks to the substrate or bounces back depends on the degree and rate of plastic deformation of particle/substrate interface (Ref 15). During particle impacting and deformation processes, an initial partial bonding between the particle and substrate is probably achieved; however, such ''immature'' bonding is also probably broken up by excessively high springback forces due to an insufficient fraction of bonded areas. Such detachment could be attributed to a very short contact time or a very high tensile force caused by a high tangential component of momentum of the particle in the case of, for example, the particle impinging at an angle (Ref 12).

The sign of ever-bonded area shown in Fig. 8(c) means that the shear instability and temperature rise has occurred when the particle impinged on the substrate causing the local metallic bonding between the exposed

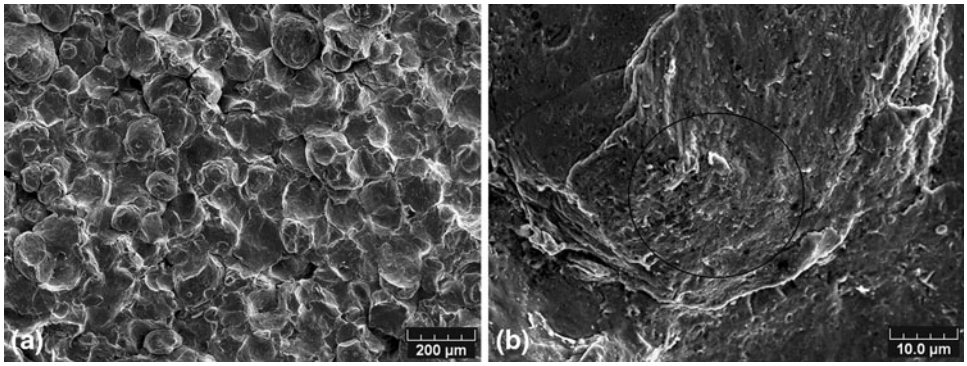


**Fig. 9** Surface morphology of the coating (a) and high magnification of an adhered particle (b)

fresh metal; however, owing to the large rebounding energy of the particle, the adhered metal was torn apart. This fact proves further that shear instability can occur even for the rebounded particles. As mentioned above, shear instability does not necessarily cause particle bonding. Thus, the question of whether the critical velocity of a given particle coincides with the occurrence of adiabatic shear instability (Ref 15) now becomes more confusing, and it, therefore, necessarily requires further investigation. For coating deposition, it is known that the successive impacting of the subsequent particles enhances the coating, and the particles experience the multi-impacting from different particles bonded or unbonded. Figure 9 shows the surface morphology of the deposited coating. Besides the deformed particles and the obvious craters, the local zones at the particle surfaces also experienced shearing by the rebounded particles as shown in Fig. 9(b) marked by the circle.

**3.2.3 Cross Sections.** In the following, some results on cross sections of the single impacts and coating are provided to further analyze the particle impacting behavior. Figure 10 shows representative micrographs of the cross sections of the single impacts and coatings. Under this high-temperature gas condition, the resultant coating was thick. According to the observation of the single impacts (Fig. 8a), many particles were bonded to the substrate. As shown in Fig. 10(a), the larger adhered particle is estimated to have a flattening ratio of about 1.4, and a compression ratio of 19.8% with the equivalent starting diameter of about 67 μm. It should be noted that the flattening ratio and the compression ratio given here are just cursory evaluations rather than a precise calculation, because an exactly bisected particle is difficult to be ensured during the sample cutting process. Based on the particle velocity distribution in this study and the simulation work in the previous study (Ref 11), the flattening ratios are comparable to the previously reported ones but the compression ratios are a little lower (about 30%). The difference may result from the estimation of the apparent particle diameter from the cross section. Further study is necessary to reveal the underlying reason.

From the coating cross sections (Fig. 10b), it is clearly seen that the deposited particles have experienced more plastic deformation than the single impacts and well flattened under the tamping effect of the successive impacting particles no matter if they are bonded or nonbonded. Compared with single impacts, particles in coating deposition are exposed to a high temperature for longer duration, and those already bonded particles can experience a heavier deformation exerted by the impacting of subsequently arriving particles (Ref 16). In Fig. 10(b), some obvious cracks were observed, which may be generated during coating deposition. This means that the high velocity impacting of the particle will also influence the bonding of the previously deposited particles. This is also why the cold-sprayed coatings have relatively high compressive residual stresses (Ref 18).

When observed in the etched state (Fig. 10c, d), the interfaces between the deposited particles and between the particles and the substrate are clearly present. This may mean that the weak interfaces are readily eroded (Ref 19). It is noteworthy that besides the changed interfacial grains, the fine twins within the particles resulting from the intense impacting are present. It is clearer at a high magnification (Fig. 10e). The deformation twining has been investigated under dynamic plastic deformation (Ref 20) and shock-induced deformation (Ref 21). Coarse copper particles have been used in this study as previously indicated; however, this may have an influence on its dynamic recrystallization. Assadi et al. indicated that particle size may have an effect on the heat conduction rate (Ref 12). Schmidt et al. (Ref 6) indicated that the cooling rate decreases with increasing the particle size. Coarse particles can have a lower cooling rate due to lower temperature gradient within it. They pointed out that the lower heat transfer rate in coarser particles can promote the occurrence of localized shear instability. Maximum interface temperature in coarser particles can even be close to the melting temperature of material because of a lower cooling rate and a longer time exposed to high temperature (Ref 6). On the other hand, coarse particles may have a relatively lower viscous shear strength in the jetting region, a lower strain-rate hardening, a lower strength due to a lower quench rate during powder production, and a lower oxygen content due to their lower surface to volume ratios; all these influences

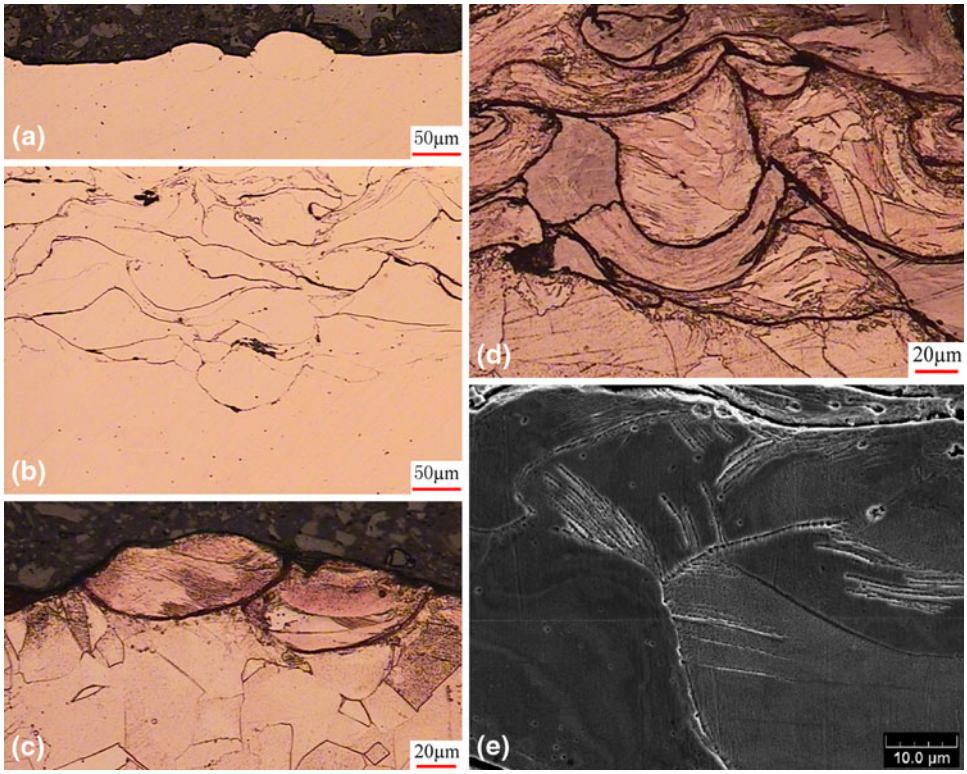


**Fig. 10** OM micrographs of cross-sections of the single impacts (a, c) and coating (b, d). (e) SEM micrograph of the coating at high magnification. (c, d, e) are in the etched state

can ultimately decrease its critical velocity compared to small particles (Ref 6). The strain rates have already been estimated to be ranging from $10^2$ to $10^3$ l/s (Ref 20), and ~$10^6$ l/s (Ref 21). However, as reported in the literature, the maximum strain rate during cold spraying can even reach $10^9$ l/s (Ref 6) because of a ''burst'' deformation in the early stages of impact (Ref 16). With the above mentioned analysis being into account, dynamic recrystallization are more prone to occur within coarser particles which have higher strain rates in cold spraying. Through the dynamic recrystallization, the high strain energy induced by severe deformation of particles can be relieved by forming subgrains (Ref 16).

The occurrence of twins presented in Fig. 10 can be considered as a result of high strain rate deformation near the interface zones. Twinning is common in cold-sprayed copper particles because only a moderate level of strain rate is required for twinning in coarse-grained copper, which can be easily satisfied considering the characteristic of cold spraying. Twinning and refinement of grains of cold-sprayed copper particles have been extensively studied by King et al. (Ref 16).

### 3.3 Microhardness

The particle properties will influence the particle deposition (Ref 4); therefore, the microhardness of the powders and the coatings were investigated and are shown in Fig. 11. The microhardness of the starting powder and the annealed substrate was also given in Fig. 11. The annealed particles (No. 2 in Fig. 11) present a little lower hardness than the starting particles (No. 1) owing to the

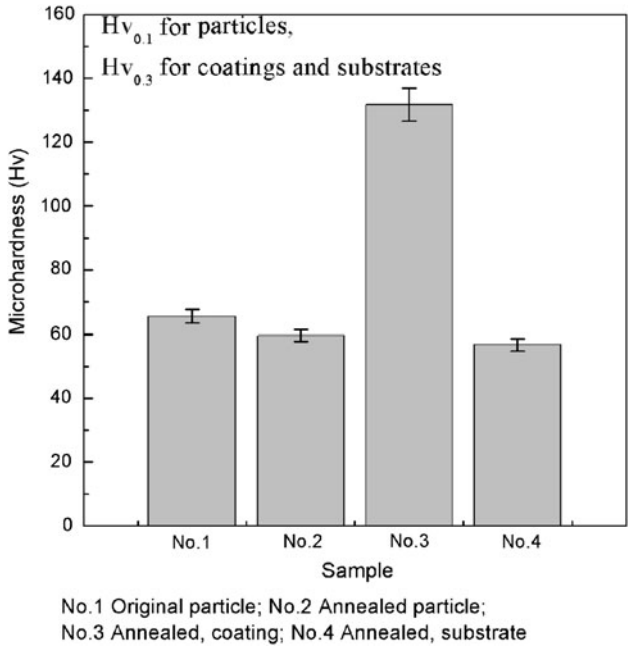


**Fig. 11** Microhardness of particles, coatings, and substrates in different cases

complete annealing effect. For the annealed substrate, its hardness is similar to the annealed Cu bulk (Ref 19), but much lower than the rolled Cu substrate. It is clearly seen that the deposited coatings (No. 3) show much higher hardness due to the strain-hardening effect by the high velocity impact of particles during cold spraying (Ref 2, 19). The coating hardness is comparable to the reported values obtained under other spray conditions (Ref 2, 19).

## 4. Concluding Remarks

Based on the results obtained in this study, it is found that the annealing treatment softens the spray particles and the substrate, and thus is beneficial to particle deformation and bonding. The sizes of the rebounded particles are apparently increased compared to the starting powders because of the rebound of the larger particles and the intensive plastic deformation of particles. For the deposited particles, obvious plastic deformation of particles has occurred which caused the higher hardness of the coating. It has been found in this study that the rebounded particles also experienced large deformation and shear instability at the impact interfaces. This will necessitate a further study on the detailed relationship between the critical velocity and the shear instability of particles, possibly with the Focused-Ion-Beam Scanning Electron Microscopy (FIB/SEM) and high resolution TEM or numerical simulations to reveal the bonding nature of cold sprayed particles.

### Acknowledgments

This study was partially supported by the Ao-Xiang Star Project of NPU (Northwestern Polytechnical University), and the Program for New Century Excellent Talents in University by the Ministry of Education of the People's Republic of China and the 111 Project (B08040).

### References

1. A. Papyrin, Cold Spray Technology, *Adv. Mater. Proc.*, 2001, **159**, p 49-51
2. T. Stoltenhoff, H. Kreye, and H.J. Richter, An Analysis of the Cold Spray Process and Its Coatings, *J. Therm. Spray Technol.*, 2002, **11**, p 542-550
3. R.C. Dykhuizen, M.F. Smith, D.L. Gilmore, R.A. Neiser, X. Jiang, and S. Sampath, Impact of High Velocity Cold Spray Particles, *J. Therm. Spray Technol.*, 1999, **8**, p 559-564
4. H. Assadi, F. Gärtner, T. Stoltenhoff, and H. Kreye, Bonding Mechanism in Cold Gas Spraying, *Acta Mater.*, 2003, **51**, p 4379-4394
5. M. Grujicic, C.L. Zhao, W.S. DeRosset, and D. Helfritch, Adiabatic Shear Instability Based Mechanism for Particles/Substrate Bonding in the Cold-Gas Dynamic-Spray Process, *Mater. Des.*, 2004, **25**, p 681-688
6. T. Schmidt, F. Gärtner, H. Assadi, and H. Kreye, Development of a Generalized Parameter Window for Cold Spray Deposition, *Acta Mater.*, 2006, **54**, p 729-742
7. C.J. Li, W.Y. Li, and H.L. Liao, Examination of the Critical Velocity for Deposition of Particles in Cold Spraying, *J. Therm. Spray Technol.*, 2006, **15**, p 212-222
8. W.Y. Li, H.L. Liao, C.J. Li, H.-S. Bang, and C. Coddet, Numerical Simulation of Deformation Behavior of Al Particles Impacting on Al Substrate and Effect of Surface Oxide Films on Interfacial Bonding in Cold Spraying, *Appl. Surf. Sci.*, 2007, **253**, p 5084-5091
9. K. Kang, S. Yoon, Y. Ji, and C. Lee, Oxidation Dependency of Critical Velocity for Aluminum Feedstock Deposition in Kinetic Spraying Process, *Mater. Sci. Eng. A*, 2008, **486**, p 300-307
10. M. Grujicic, J.R. Saylor, D.E. Beasley, W.S. DeRosset, and D. Helfritch, Computational Analysis of the Interfacial Bonding Between Feed-Powder Particles and the Substrate in the Cold-Gas Dynamic-Spray Process, *Appl. Surf. Sci.*, 2003, **219**, p 211-227
11. W.Y. Li, H.L. Liao, C.J. Li, G. Li, C. Coddet, and X.F. Wang, On High Velocity Impact of Micro-sized Metallic Particles in Cold Spraying, *Appl. Surf. Sci.*, 2006, **253**, p 2852-2862
12. H. Assadi, F. Gärtner, T. Stoltenhoff, and H. Kreye, Application of Analytical Methods for Understanding and Optimization of Cold Spray Process, *Proceedings of the 6th High-Velocity Oxy-Fuel Flame Spraying (HVOF) Colloquium*, P. Heinrich, Ed., November 27-28, 2003 (Erding, Germany), Gemeinschaft Thermisches Spritzen e.V., 2003
13. W.-Y. Li, C. Zhang, C.-J. Li, and H.L. Liao, Modeling Aspects of High Velocity Impact of Particles in Cold Spraying by Explicit Finite Element Analysis, *J. Therm. Spray Technol.*, 2009, **18**, p 921-933
14. W.-Y. Li, H.L. Liao, G. Douchy, and C. Coddet, Optimal Design of a Cold Spray Nozzle by Numerical Analysis of Particle Velocity and Experimental Validation with 316L Stainless Steel Powder, *Mater. Des.*, 2007, **28**, p 2129-2137
15. C. Borchers, F. Gärtner, T. Stoltenhoff, H. Assadi, and H. Kreye, Microstructural and Macroscopic Properties of Cold Sprayed Copper Coatings, *J. Appl. Phys.*, 2003, **93**, p 10064-10070
16. P.C. King, S.H. Zahiri, and M. Jahedi, Microstructural Refinement within a Cold-Sprayed Copper Particle, *Metall. Mater. Trans. A*, 2009, **9**, p 2115-2123
17. K.B. Yin, Y.D. Xia, C.Y. Chan, W.Q. Zhang, Q.J. Zhang, X.N. Zhao, and A.D. Li, The Kinetics and Mechanism of Room-Temperature Microstructural Evolution in Electroplated Copper Foils, *Scripta Mater.*, 2008, **58**, p 65-68
18. S. Sampath, X.Y. Jiang, J. Matejicek, L. Prchlik, A. Kulkarni, and A. Vaidya, Role of Thermal Spray Processing Method on the Microstructure, Residual Stress and Properties of Coatings: An Integrated Study for Ni-5 wt.%Al Bond Coats, *Mater. Sci. Eng. A*, 2004, **364**, p 216-231
19. W.-Y. Li, C.-J. Li, and H. Liao, Effect of Annealing Treatment on the Microstructure and Properties of Cold-Sprayed Cu Coating, *J. Therm. Spray Technol.*, 2006, **15**, p 206-211
20. C.S. Hong, N.R. Tao, K. Lu, and X. Huang, Grain Orientation Dependence of Deformation Twinning in Pure Cu Subjected to Dynamic Plastic Deformation, *Scripta Mater.*, 2009, **61**, p 289-292
21. F. Cao, I.J. Beyerlein, F.L. Addessio, B.H. Sencer, C.P. Trujillo, E.K. Cerreta, and G.T. Gray, Orientation Dependence of Shock-Induced Twinning and Substructures in a Copper Bicrystal, *Acta Mater.*, 2010, **58**, p 549-559